

SLAC - PUB - 4328
May 1987
(E)

Preliminary Results on B^0 - \bar{B}^0 Mixing from MAC*

Roger Hurst

Stanford Linear Accelerator Center
Stanford, CA 94305

and

University of Houston
Houston, TX 77004

Representing the MAC Collaboration ^[a]

An excess of like-charge dimuons has been observed with the MAC detector in multihadron events produced in e^+e^- annihilation at $\sqrt{s} = 29$ GeV. If this excess is attributed to B^0 - \bar{B}^0 mixing, the corresponding value of the mixing parameter $\chi = \Gamma(B \rightarrow \mu^- X) / \Gamma(B \rightarrow \mu^\pm X)$ is $\chi = 0.21_{-0.15}^{+0.25}$ and $\chi > 0.02$ at 90% C.L.

Invited talk presented at the XXIInd Rencontres de Moriond:

Electroweak Interactions and Unified Theories

Les Arcs, France, March 8-15, 1987

* This work was supported in part by the U. S. Department of Energy under contract number DE-AC03-76SF00515 and by the National Science Foundation under grant number NSF-PHY82-15133.

Immediately after the discovery of the beauty quark^[1] speculation began that significant mixing might occur between $B^0 \leftrightarrow \bar{B}^0$ just as it does between $K^0 \leftrightarrow \bar{K}^0$.^[2] UA1 and Argus have recently reported evidence for such mixing.^[3] The MAC collaboration has performed a measurement of B^0 - \bar{B}^0 mixing using data collected at the PEP storage ring. At PEP e^+e^- collisions with $\sqrt{s} = 29$ GeV provide a favorable environment for studying B^0 - \bar{B}^0 mixing. In contrast with $p\bar{p}$ collisions the $e^+e^- \rightarrow b\bar{b}$ differential cross section is very well known and the events are quite clean. And unlike e^+e^- collisions at the $\Upsilon(4s)$ resonance PEP energy is well above the threshold for producing B_s^0 mesons, the species thought most likely to exhibit significant mixing,^[4] and the energy is sufficient to produce a clear jet structure with the decay products of the b and \bar{b} isolated from each other in opposite jets.

To measure B^0 - \bar{B}^0 mixing MAC uses multihadron events containing two muons. The muons provide flavor enrichment and they also provide charge tagging to discriminate between the decays $b \rightarrow \mu^- \bar{\nu}_\mu c$ and $\bar{b} \rightarrow \mu^+ \nu_\mu \bar{c}$. Without mixing prompt dimuons in $e^+e^- \rightarrow b\bar{b}$ events have opposite charges, with mixing there is some probability of producing like-charge prompt dimuons. Like-charge backgrounds come from events in which one of the muons is produced from the cascade decay $b \rightarrow c \rightarrow \mu^+$ or $\bar{b} \rightarrow \bar{c} \rightarrow \mu^-$ and from events in which a like-charge hadron is misidentified as a muon.

An event with two identified muons in the MAC detector^[5] is shown in Fig. 1. Muons are identified over 95% of the solid angle by requiring: (1) consistent measurements of the muon momentum vector from independently reconstructed inner and outer drift chambers which are separated by more than 5 absorption lengths of hadron calorimetry; (2) energy deposition in the hadron calorimeter consistent with the passage of a minimum ionizing particle; (3) p between 2 and 10 GeV/c where p is the weighted average of the two independent momentum measurements; (4) $p_\perp/p > 0.1$ to cut out the fake muon background in the core of the jet. Muon p_\perp is calculated relative to the thrust axis, an estimator of the original quark direction. The thrust axis is determined from energy deposition in the calorimeters with muon-associated calorimeter hits augmented to correspond to the measured muon momentum. To have greater assurance of the reliability of the thrust axis recon-

struction events are rejected if thrust is less than 0.72 or if the thrust axis is within 30° of the beam axis. The success of muon identification criteria may be judged by the probability of misidentifying a hadron as a prompt muon. Hadrons which either penetrate the calorimeters or decay into secondary muons may fake prompt muons. Using taus which decay into three charged particles as a clean source of hadrons and all of the cuts listed above except the p_\perp/p cut, the misidentification probability is found to be $(0.41 \pm 0.08)\%$ for tau data and $(0.35 \pm 0.03)\%$ for tau Monte Carlo. The agreement indicates that the data is modeled well by the Monte Carlo. This small misidentification probability is further reduced by the p_\perp/p cut.

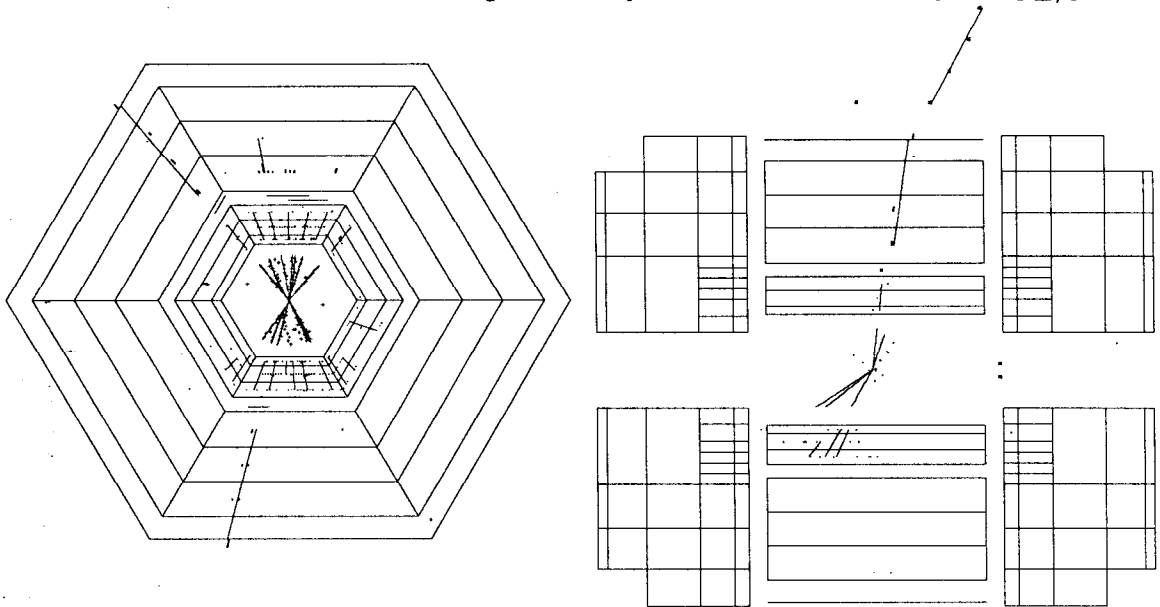


Fig. 1. Dimuon event in the MAC detector.

The full MAC data sample of $310 pb^{-1}$ is used for this analysis. The above muon selection criteria yield 2813 single muon events with 2790 ± 53 predicted by the Monte Carlo. There are 47 dimuon events with 51 ± 5.6 predicted. The data is modeled with the Lund Monte Carlo (version 5.2) and EGS and HETC^[6] are used to simulate the passage of every particle through the detector. Monte Carlo predictions are largely based on $\sim 2800 pb^{-1}$ of generated beauty and charm dimuon events. However, predictions for background events which contain one or more fake muons are made from $307 pb^{-1}$ of generated multihadrons of all flavors and types. Agreement between the data and Monte Carlo is illustrated by the p and p_\perp spectra in Figure 2.

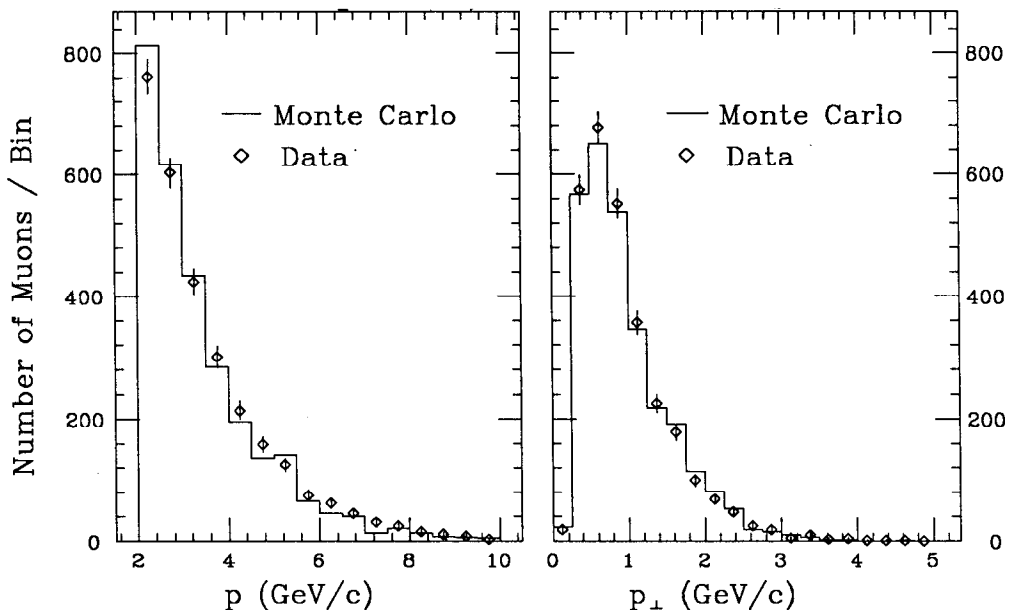


Fig. 2. Momentum and transverse momentum spectra of single muons.

High p_{\perp} is characteristic of prompt muons from b decays.^[7] Figure 3 shows a Monte Carlo simulation of the effectiveness of a p_{\perp} cut for selecting a data sample enriched in $b\bar{b}$ events. The upper (dimuon) curve approaches 100% for $p_{\perp} > 1.0$ GeV/c.

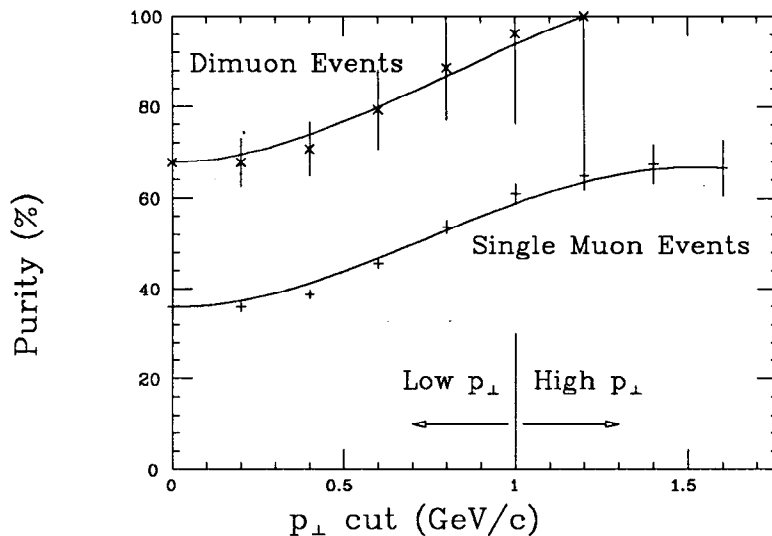


Fig. 3. Flavor purity of sample.

Dividing p_{\perp} into 'lo' (< 1 GeV/c) and 'hi' (≥ 1 GeV/c) regions, the data is partitioned into three bins—a 'lo-lo' bin with $p_{\perp} < 1$ for both muons, a 'lo-hi' bin with $p_{\perp} \geq 1$ for only one muon, and a 'hi-hi' bin with $p_{\perp} \geq 1$ for both muons. The 'hi-hi' bin has the greatest purity of $b\bar{b}$ events. Events are divided into two

jets by a plane perpendicular to the thrust axis and are classified as ‘same-jet’ or ‘opposite-jet’ depending on the positions of the two muon tracks. The table below shows numbers of dimuon events and Monte Carlo predictions according to this classification. The data agrees well with the predictions. The predicted numbers of events and their errors are scaled to data luminosity, but Poisson fluctuations on the numbers of predicted events are not included.

Numbers of Dimuon Events
Data (Monte Carlo in parentheses)

p_{\perp} bin	Same Jet	Opposite Jet	Total
Lo-Lo	1 (1.5 ± 1.0)	11 (10.2 ± 1.9)	12 (11.7 ± 2.1)
Lo-Hi	4 (4.9 ± 1.5)	11 (16.3 ± 2.7)	15 (21.2 ± 3.1)
Hi-Hi	8 (7.6 ± 2.1)	12 (10.5 ± 1.4)	20 (18.1 ± 2.5)
Total	13 (14 ± 2.8)	34 (37 ± 3.6)	47 (51 ± 4.6)

The significant quantities in a mixing measurement are the relative numbers of like-charge and unlike-charge dimuons in opposite jets. Same-jet dimuons contain no information about mixing but are a good check on the modeling of backgrounds. The table below shows data and Monte Carlo predictions without mixing. The same-jet data agrees very well with the predictions, however, the opposite-jet data shows significant deviation from the predictions. The greatest deviation is in the ‘hi-hi’ bin, exactly where mixing would most increase the number of like-charge dimuons. The probability of a statistical fluctuation of this magnitude is $\sim 5\%$.

Like and Unlike Charge Dimuons
Data (Monte Carlo in parentheses)

p_{\perp} bin	Same Jet		Opposite Jet	
	Like Charge	Unlike Charge	Like Charge	Unlike Charge
lo-lo	0 (0.5^{+7}_{-5})	1 (1.0 ± 0.7)	1 (2.7 ± 1.3)	10 (7.5 ± 1.5)
lo-hi	1 (1.0 ± 1.0)	3 (3.9 ± 1.1)	4 (5.0 ± 1.8)	7 (11.3 ± 2.0)
hi-hi	1 (2.0 ± 1.4)	7 (5.6 ± 1.5)	5 (1.9 ± 0.8)	7 (8.6 ± 1.2)
Total	2 (3.5 ± 1.9)	11 (10.5 ± 2.0)	10 (9.6 ± 2.4)	24 (27.4 ± 2.8)

The fraction $F = (\text{number of like-charge dimuons})/(\text{total dimuons})$ is plotted in Figure 4a. We see reasonable agreement between data and Monte Carlo for same-jet dimuons (the three p_{\perp} bins combined) and for the first two bins of opposite-jet dimuons, but a discrepancy of $\sim 2\sigma$ in the opposite-jet ‘hi-hi’ bin. Figure 4b shows the sensitivity to mixing defined by $S = (U_B - L_B)/Total$ where U_B and L_B are the predicted numbers of unlike-charge and like-charge beauty dimuons without mixing. The large value of S for the ‘hi-hi’ bin suggests mixing as a natural explanation for the excess of like-charge dimuons in the data.

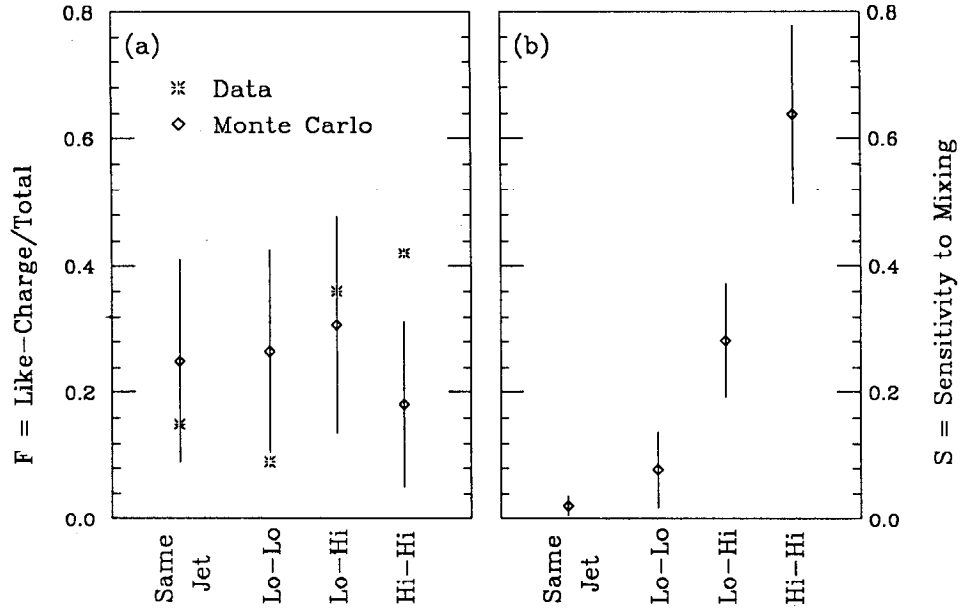


Fig. 4. Fraction of Like-Charge Dimuon Events and Sensitivity to Mixing.

To describe the amount of mixing we define

$$f = 2\chi(1 - \chi) \quad (1)$$

$$\text{where } \chi = \frac{\Gamma(B \rightarrow \mu^- X)}{\Gamma(B \rightarrow \mu^\pm X)} = \frac{\text{'wrong' sign decays}}{\text{'right' + 'wrong' sign}} \quad (2)$$

and B represents an average over the beauty particles in the sample (B_u^\pm , B_d^0 , B_s^0 , Λ_b ...). χ is the fraction of prompt muons which change sign as a result of mixing, whereas f is the fraction of dimuon events which change relative sign as a result of

mixing. The parameters F , S , and f are related by

$$F_{\text{mixing}} = F_0 + fS \quad (3)$$

where F_0 is the Monte Carlo prediction with zero mixing and F_{mixing} is the value of F calculated for any given amount of mixing, f . If we attribute the ‘hi-hi’ bin deviation to mixing, we can use Eq. 3 to calculate the amount of mixing

$$F_{\text{data}} = F_0 + fS \implies f = 0.37^{+0.23}_{-0.21}$$

To fit all three bins in an unbiased way we maximize the log likelihood

$$\ln \mathcal{L}(f) = \sum_i L_i \ln(F_{0i} + fS_i) + U_i \ln[1 - (F_{0i} + fS_i)] \quad (4)$$

where L_i and U_i are the numbers of like and unlike charge data dimuons in bin i . The log likelihood is plotted in Figure 5 with Monte Carlo uncertainties folded in and from it we determine the result

$$f = 0.34 \pm 0.22 \quad f > 0.04 \text{ at } 90\% \text{ C.L.}$$

$$\text{or equivalently } \chi = 0.21^{+0.25}_{-0.15} \quad \chi > 0.02 \text{ at } 90\% \text{ C.L.}$$

Within large statistical uncertainty MAC data favors non-zero mixing and puts a limit on the likely value of mixing parameters.

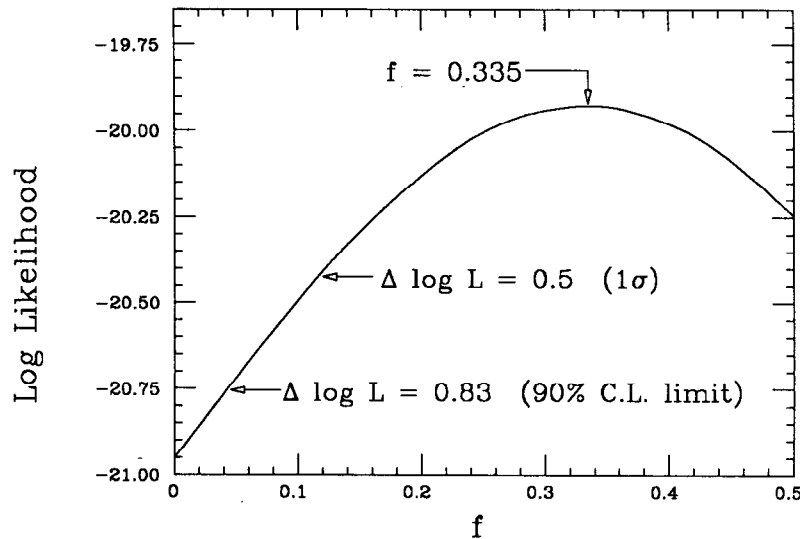


Fig. 5. Log Likelihood of f .

It has become common practice to plot results of mixing experiments in terms of 90% confidence level limits on the parameters r_s and r_d ^[8] which are related to χ by

$$r_i = \frac{\chi_i}{1 - \chi_i} \quad \text{and} \quad \chi = p_s \chi_s + p_d \chi_d \quad (5)$$

where p_i = proportion of B_i^0 in the sample and where equal semileptonic branching ratios are assumed for all beauty hadrons. Figures 6a and 6b show such plots for all experiments currently reporting results on B^0 - \bar{B}^0 mixing.^[8] The Mark II, UA1, and MAC contours depend on untested assumptions about event sample composition; $(p_s, p_d) = (0.2, 0.4)$ is assumed for Fig. 6a and $(p_s, p_d) = (0.1, 0.35)$ is assumed for Fig. 6b. The intersection of the allowed regions of all experiments (not 90% C.L.!) is shaded. If this area is taken as the allowed region of parameter space, substantial mixing is indicated. The allowed region in Fig. 6a conflicts with the theoretical expectation^[4] that $r_s \gg r_d$, i.e. that mixing should be much greater for B_s^0 than for B_d^0 . However, that conflict does not exist with the composition assumed in Fig. 6b.

I thank T. L. Lavine, F. Muller, H. N. Nelson, and D. M. Ritson for their help preparing this talk.

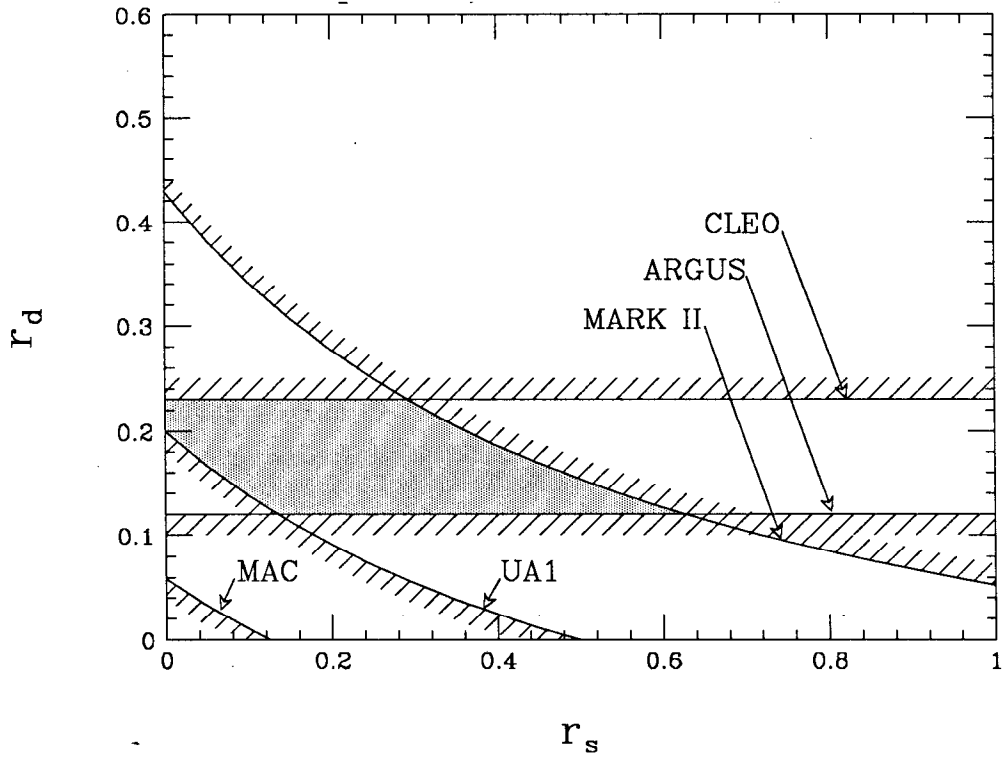


Fig. 6a. Experimental 90% C.L. limits on mixing for $(p_s, p_d) = (0.2, 0.4)$.

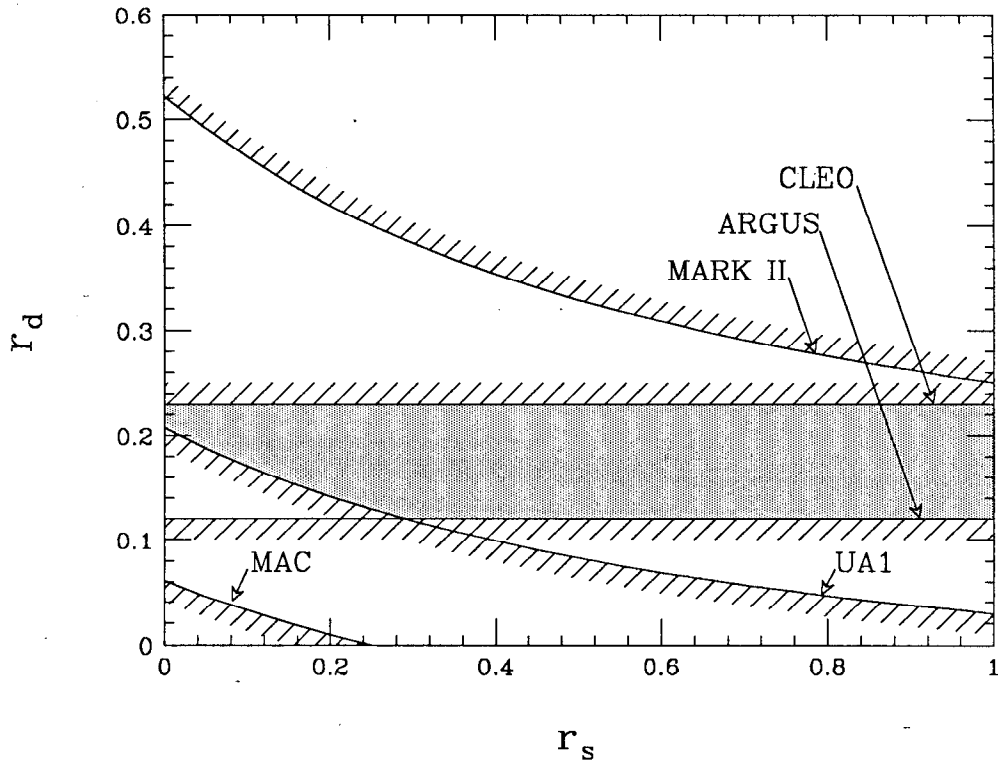


Fig. 6b. Experimental 90% C.L. limits on mixing for $(p_s, p_d) = (0.1, 0.35)$.

REFERENCES

(a) The MAC collaboration consists of:

W. W. Ash, H. R. Band, T. Camporesi, G. B. Chadwick, M. C. Delfino, R. De Sangro, W. T. Ford, M. W. Gettner, G. P. Goderre, D. E. Groom, R. B. Hurst, J. R. Johnson, K. H. Lau, T. L. Lavine, R. E. Leedy, T. Maruyama, R. L. Messner, J. H. Moromisato, L. J. Moss, F. Muller, H. N. Nelson, I. Peruzzi, M. Piccolo, R. Prepost, J. Pyrlik, N. Qi, A. L. Read, Jr., D. M. Ritson, L. J. Rosenberg, W. D. Shambroom, J. C. Sleeman, J. G. Smith, J. P. Venuti, P. G. Verdini, E. von Goeler, R. Weinstein, D. E. Wisner, and R. W. Zdarko.

University of Colorado, INFN Frascati, University of Houston, Northeastern University, Department of Physics and SLAC, Stanford University, University of Utah, University of Wisconsin.

1. S.W. Herb *et al.*, *Phys. Rev. Lett.* **39** (1977) 252.
2. J. Ellis *et al.*, *Nucl. Phys.* **B131** (1977) 285.
3. T. Schaad *et al.* (Mark II Collaboration), *Phys. Lett.* **160B** (1985) 188;
A. Bean *et al.* (CLEO Collaboration), *Phys. Rev. Lett.* **58** (1987) 183;
C. Albajar *et al.* (UA1 Collaboration), preprint CERN-EP/86-209 (1986);
H. Schröder (Argus Collaboration) talk at this conference.
Note that the 90% C.L. limits shown in Fig. 6 for Argus and UA1 are 1.29σ from their reported results.
4. A. Ali, preprints DESY 85-107 and DESY 86-108.
5. For a description of the MAC detector see E. Fernandez *et al.*, *Phys. Rev.* **D31** (1985) 1537.
6. Electromagnetic showers were simulated by the EGS code, described in R. L. Ford and W. R. Nelson, SLAC Report No. SLAC-210, 1978 (unpublished); and hadron cascades by HETC, described in the report of T. W. Armstrong in *Computer Techniques in Radiation Transport and Dosimetry*, edited by W. R. Nelson and T. M. Jenkins (Plenum, New York, 1980)
7. E. Fernandez *et al.* (MAC Collaboration), *Phys. Rev. Lett.* **50** (1983) 2054.
8. A. Pais and S. B. Treiman, *Phys. Rev.* **D12** (1975) 2744.